bswarna261@gmail.com;

DOI: 10.21062/mft.2025.053 © 2025 Manufacturing Technology. All rights reserved.

http://www.journalmt.com

# AI-Integrated Thermal Prediction and Multi-Criteria Optimization in Cylindrical Grinding Using Machine Learning and Genetic Algorithms

Maya M. Charde<sup>1</sup>, Yogesh J. Bhalerao<sup>1</sup>, Lenka Cepova (0000-0002-7328-9445)<sup>2</sup>, Sharadchandra N. Rashinkar<sup>3</sup>, B. Swarna<sup>4</sup>

<sup>1</sup>Department of Mechanical Engineering, MIT Academy of Engineering, Alandi (D), Pune 412105, India. E-mail: mmcharde@mitaoe.ac.in, ybhalerao@mitaoe.ac.in

<sup>2</sup>Department of Machining, Assembly and Engineering Metrology, Faculty of Mechanical Engineering, VSB-Technical University of Ostrava, 70800 Ostrava, Czech Republic. E-mail: lenka.cepova@vsb.cz

<sup>3</sup>Dr D Y Patil School of MCA, Charholi (Bk), Pune 412105, India. E-mail: sharadrashinkar0106@gmail.com <sup>4</sup>University Centre for Research & Development, Chandigarh University, Mohali 140413, India.

The paper focuses on the application of machine learning techniques and optimization algorithms in predictions and controls of grinding temperature variations. The major thrust of investigation has been on how the different input conditions such as feed, depth of cut, and cooling conditions influence grinding temperatures and the effectiveness of these conditions on the control of their thermal effects. Three machine learning models: Random Forest (RF), Gradient Boosting (GB), and Artificial Neural Networks

on how the different input conditions such as feed, depth of cut, and cooling conditions influence grinding temperatures and the effectiveness of these conditions on the control of their thermal effects. Three machine learning models: Random Forest (RF), Gradient Boosting (GB), and Artificial Neural Networks (ANN) were then used to develop prediction models for the grinding temperature on both face and shoulder of the workpiece. Out of all the models, RF achieved a much higher R² score of 0.96 as compared to both GB and ANN, indicating its greater predictive performance. Furthermore, Bayesian optimization and genetic algorithms were employed in model optimization and grind parameters and cooling condition optimization to avoid damages caused due to temperature. MQL has been found to be highly superior to the inefficient dry cooling methods in terms of achieving lower grinding temperatures and, therefore, seems to be most suited as an eco-friendly yet practical cooling solution as based on this comparison. Altogether, these research findings indicate that AI-based techniques and traditional optimization methods can lead to much better grinding in terms of efficiency and energy consumption, as well as surface quality, and assist towards greener manufacturing altogether.

**Keywords:** Cylindrical Grinding, Machine Learning, Random Forest, Gradient Boosting, Artificial Neural Networks, Temperature Prediction, Optimization Algorithms, Cooling Conditions

### 1 Introduction

Grinding technology is extensively applied in manufacturing industries, e.g., composites, aerospace alloys, and wind turbine blades, and its machining accuracy directly affects the working performance and surface integrity of workpieces [1]. While grinding processes produce surface thermomechanical damages in hard components owed to high frictional heat, these damages lead to the formation of tensile residual stresses, lowered hardness, rehardening, and micro-cracking, which demand the development of a reliable damage detection method [2]. Grinding, one of the most important processes for obtaining good quality surfaces of steel, is influenced by the geometrical changes and changes in material properties underneath the surface, which interfere with the functionality and reliability of a component [3]. The high temperatures and mechanical stresses associated with

grinding induce thermal expansion, phase transformation, and plastic deformation in the more thin-walled workpieces, resulting in residual stresses and distortion [4]. While FE simulation is an attractive method for predicting distortion at a low cost, it does require a long time for the modeling and solving of complex nonlinear equations, which dictate thermal and mechanical effects [5]. High-end real-time measuring technologies along with Artificial Intelligence (AI) are going to reform the whole manufacturing process as they technically permit efficient collection, storage, and data analysis for process optimization. Machine Learning (ML), a specific and important aspect of AI, is extremely competent in analyses of huge, complex databases, improving the accuracies of predictions, and offering a new lease of life to the old and wellestablished processes in manufacturing at advanced levels [6].

Recent research revealed that there are still many open questions regarding the dynamics of energy partition in belt grinding and the thermal and mechanical behaviours of the grinding process. This topic is being addressed through coupling single grain scratch testing with a finite element analysis method to calculate energy distribution, yet more general models are still awaited. For instance, an effective model was proposed, which calculates the dynamic energy partition in robotic belt grinding, and verification tests have shown that an error of 17.2% concerning specific workpieces, such as SUS304 and AA6061-T6, is attainable [7]. The same improvements have been made to thermal modeling in cup wheel grinding by incorporating the geometry of wheelwork contact at which heat distribution occurs during grinding. The resultant improved model has great significance, giving errors in grinding temperature predictions below 6.6% [8]. In rail grinding, the thermal model was proposed to predict the grinding temperature and analyze the formation of white etching layers (WEL) that establish at about 400°C, but a robust model for WEL formation prediction, as well as the effects of thermal and mechanical stresses, is still required [9].

With all the thermal-induced effects of laser irradiation being integrated into the laser-assisted grinding process, much work is still left to prediction models for surface roughness and topography in LAG of zirconia ceramics. Theoretical and experimental works have shown good congruence with the surface roughness values, though further refinement of the model for temperature-dependent material properties is still needed [10]. In ultra-precision grinding, better understanding has been gained about the influences of both cutting speed and depth-of-cut on damage at the surface and below it; the cuts show improved results, such as reduced surface roughness and subsurface damage, as cutting speed increases [11]. In the manufacturing industries, like for instance the solid wood panel and concrete industries, the AIOGA optimization techniques are proven to be good at improving scheduling, thereby minimizing operational time [12]. Hybrid algorithms such as GEP-PSO have also yielded very promising developments in machining processing. They include reducing energy usage and tool wear while upholding surface quality in machining superalloys [13]. In addition, machine learning approaches like GA-BP neural networks helped make improvements in pressure monitoring for drilling applications, which will provide other pressure monitoring types of reference for future uses [14].

Applications of GMDH ANN, in conjunction with evolutionary algorithms NSGA-II, MOPSO, and MOGWO, to predict the rheological behavior of CuO

NPs, have largely succeeded. However, the Genetic Algorithm (GA) was declared to be best performing among all studied techniques [15]. Also, Inconel 690, given its heat resistance, is known for being difficult for machining, which, therefore, makes it even more important for tuning of conduct on lubrication strategies and optimization algorithms. NSGA-II, however, particularly proved to be successful, at a success rate of 82.3% against 79.1% by TLBO; hence faster and more efficient for machining optimization application [16]. Finally, the hybrid optimization approaches that combine Bayesian optimization and NGBoost have proved useful for optimizing the concrete production mix design. These advances reduce costs and carbon emissions tremendously [17]. According to the fuzzy-AHP-MOORA method applied to AISI 304 stainless steel, with trials 12, 14, and 8 occupying the 1st, 2nd, and 3rd positions based on differences of 0.2133, 0.2076, and 0.1083, respectively, bushing length undergoes the most prominent improvement [18], implying the need to select the parameters carefully for the purpose of quality control in thermal friction drilling. For grinding AISI 1060 high-speed steel, the combined effects of compressed air, MQL, and nanofluids are being investigated, with the best working mode found to be MQL combined with compressed air, where higher cutting speeds improved the surface roughness, but the cutting temperature was a trade-off [19]. In the meantime, the grinding process of W18CR4V steel was optimized using machine-learning models such as DNN-GA while also attaining about 81.5% and 77.7% reduction in Ra and Rz, respectively, wherein DNN-GA obtained an  $R^2 > 0.99$ and better optimization results via MOGWO [20]. Finally, Inconel 718's micromilling under MQL lubrication brought forth the clear effect of cutting parameters wherein depth of cut and feed per tooth had the highest effect with the optimal parameters ap = 0.010mm and fz = 0.008 mm/tooth with surface roughnessof 0.24 µm and channel depth deviation of 0.41 µm [21]. These advances further give hope that a combination of multiple optimization algorithms could solve the varied problems of manufacturing in many industries. Table 1 presents an inclusive summary of different studies with descriptions of materials, model, optimization algorithm, important findings, and results. The studies pertain to grinding processes, machining optimizations, and predictive modeling, highlighting the applications of advanced algorithms such as FEM, NSGA-II, and GA-BP. The results show that all such methods have been highly successful in optimizing energy efficiency, surface quality, and costs in respective raw materials and processes.

Tab. 1 Summary of Materials, Models, Optimization Algorithms, Key Findings, and Results from Relevant Studies

Ref. No.	Material Used	Model Used	Optimization Algorithm	Key Findings	Results
[7]	SUS304, AA6061-T6	Dynamic energy partition model	FEM, Iterative approach	The model for dynamic energy parti- tion considers grinding effects and thermal aspects, calculating energy partition in continuous grinding.	The method showed a maximum error of 17.2% for energy partition, enhancing understanding of robotic belt grinding.
[8]	Cup wheel grinding	3D analytical thermal model	FEM	The model integrates wheelwork contact geometry to predict grinding temperature distribution.	The model demonstrated <6.6% error for maximum temperature and <8.5% error for temperature location.
[9]	Rail material	Analytical thermal model	Non-uniform heat source dis- tribution	Predicts grinding temperature and analyzes the effect of surface burn and white etching layer (WEL).	The WEL forms at grinding temperatures around 400°C, with retained austenite and martensite observed on the surface.
[10]	Zirconia ce- ramics	Grinding wheel model	Stochastic pro- cess, thermal modeling	Developed a predictive model for sur- face topography in Laser-Assisted Grinding (LAG), considering laser power and material removal.	Experimental results closely matched simulations with errors in surface roughness (Rz and Ra) <8%.
[11]	Fine- grained grinding	Grinding process simulation	Experimental, interferometry analysis	Investigated surface roughness and subsurface damage under different depth-of-cut and cutting speed.	Found linear relationship between surface roughness (Ra) and SSD depth with significant reduction in SSD with increased cutting speed.
[12]	Solid wood panel	Simulation system for production	AIOGA (Adaptive Intelligent Optimization GA)	AIOGA improved scheduling for solid wood panel production by opti- mizing completion times and work- load balance.	AIOGA reduced maximum completion time by 39.60%, enhancing operational efficiency.
[13]	Inconel 690	Gene Expression Programming (GEP)	Particle Swarm Optimization (PSO)	GEP-PSO optimization reduced energy consumption, carbon emissions, cost, surface roughness, and tool wear during Inconel 690 machining.	Achieved a 20% energy reduction, 18.68% reduction in carbon emis- sions, 20.21% reduction in surface roughness, and 31.71% reduction in tool wear.
[14]	Well area X (Yinggehai Basin)	BP and GA-BP Neural Networks	Genetic Algorithm (GA)	GA-BP model outperformed BP in monitoring formation pressure during drilling, improving accuracy.	GA-BP achieved 92.89% accuracy in formation pressure monitoring, surpassing BP's 91.25%.
[15]	Nanofluids with CuO NPs	GMDH ANN	NSGA II, MOPSO, MOGWO	GMDH ANN combined with MOGWO provided the best performance in predicting viscosity of nanofluids.	Achieved optimal viscosity (µ) prediction at 0.96686 cP with optimized input parameters.
[16]	Inconel 690	Taguchi L27 or- thogonal array	NSGA-II, TLBO	NSGA-II outperformed TLBO in ma- chining optimization for Inconel 690, achieving a higher success rate and faster computation.	NSGA-II achieved 82.3% success rate, with faster computation (8.3 seconds) compared to TLBO (5.6 seconds).
[17]	Segment concrete	NGBoost, NSGA-III	Bayesian Opti- mization, NGBoost, NSGA-III	Hybrid optimization reduced segment concrete production costs and carbon emissions, improving mix proportions.	Optimal mix reduced costs by 31.64 yuan and carbon emissions by 31.04 kg per cubic meter, with an 11.5% improvement over experimental optimization.
[18]	AISI 304 stainless steel	Fuzzy-AHP- MOORA method	Analytic Hierar- chy Process (AHP), Fuzzy framework	The best parameters were selected for thermal friction drilling using fuzzy-AHP-MOORA.	Experimental trials 12, 14, and 8 were found to achieve the best positions, with improved response for bushing length.
[19]	AISI 1060 high-speed steel	Horizontal Spin- dle Surface Grinder	Entropy-based TOPSIS, VIKOR	MQL with compressed air and nano- particles showed the best perfor- mance, with improved surface finish.	At higher cutting speeds, better surface finish was achieved, with varying cutting temperature.
[20]	W18CR4V steel	Deep Neural Net- works (DNN), K- Nearest Neigh- bors (KNN), De- cision Trees (DT), Support Vector Machines (SVM)	Genetic Algorithm (GA), Multi-Objective Grey Wolf Optimization (MOGWO)	DNN-GA model achieved significant reduction in surface roughness and production time.	Ra reduced to 0.341 µm, Rz to 2.3 µm, and production times were optimized between 1181 to 1426 s.
[21]	Inconel 718 superalloy	Micromilling process	Taguchi method, TOPSIS	Depth of cut and feed per tooth sig- nificantly influence cutting force and surface roughness.	Optimal cutting parameters resulted in a channel depth deviation of 0.41 μm, burr formation height of 6 μm, and surface roughness of 0.24 μm.

There has been a limited number of studies investigating dynamic energy partitioning in belt grinding with specific emphasis on integrating thermal and grinding effects. Most of the thermal models that have been developed for cup wheel grinding ignore the effect of geometry of contact between wheel and workpieces. Thus, heat transfer assumptions have been overly simplified. The same situation is given when concerning rail grinding, in that, there are few studies that can accurately predict the formation of the white etching layers (WEL) and study their combined effects with thermal and mechanical stresses. However, there is room for improvement in modelling surface roughness while laser assisted grinding (LAG) and ultra-precision grinding. Further investigation is needed on hybrid optimization techniques so that they reduce inefficiencies, optimize material use, and minimize carbon emissions, especially for scheduling in some industries like solid wood panel production and concrete manufacturing. This study, therefore, aims at addressing such gaps; they include predicting temperature variations during grinding, AI-based optimization to minimize temperature rise, and comparative studies on cooling conditions, Dry and Minimum Quantity Lubrication (MQL). In addition, the research shall entail the integration of machine learning models such as Random Forest (RF), Gradient Boosting (GB), and Artificial Neural Networks (ANN), which will further enhance prediction accuracy and optimization of the grinding process. These machine learning models will offer a basis of understanding how cooling methods influence thermal stresses and surface quality, all of which ultimately bring about sustainable and efficient manufacturing processes. This study will fill existing gaps in dynamic energy partitioning and cooling optimization in advanced grinding processes such as LAG and ultra-precision grinding.

### 2 Materials and Experimental Setup

### 2.1 Workpiece Material and Specifications

The material used for the workpieces for cylindrical grinding experiments was EN31 steel, which is knowing for its hardness at 50 HRC and for having wear resistance. Its chemical composition included Carbon (1%), Chromium (1.40%), Manganese (0.50%), and others as alloying elements. Specimens were prepared by facing, turning, and step turning, followed by deep oil hardening. Holes were made by Electrical Discharge Machining (EDM) for embedding thermocouples to measure the temperature. A specially designed test rig with slip rings was made to take care of proper temperature sensing and rotation during grinding.

### 2.2 Grinding Conditions and Process Parameters

#### 2.2.1 Control Parameters

The four major parameters of the machining process determined to be in focus for this study were subsequently investigated to understand their effect on cylindrical grinding performance. The selected parameters varied from 0.025 mm to 0.04 mm for the depth of cut and were directly proportional to the amount of material removed per pass; the rate of feed that was taken into account, especially concerning the material removal rate and surface finish; the work speed, whose variations were 100-250 rpm, and it was said to be in favour of keeping the right balance of heat generation and wear rate of the grinding wheel; similarly, the wheel speed was maintained between 948 rpm and 1186 rpm and exerted a great influence on the size of abrasive chips and the subsequent thermal effect on the workpiece. In an ordered approach, the investigation established a systematic method of analysis of these parameters through the Taguchi L29 orthogonal array as the experimental design for an effective investigation of combinations of parameters by conducting 29 designed experiments. The optimization approach was based on the Smaller-the-better quality objective, aiming toward minimizing the critical output responses like temperature and surface roughness to render the grinding process much more upgraded in terms of its quality and integrity.

### 2.2.2 Cooling Methods

The investigation involved grinding experiments performed under three different cooling conditions to analyse the effect of thermal performance and surface integrity. The first cooling condition was dry grinding with no cooling, which poses a great risk of thermal damage due to excessive heat generation during grinding. Second condition is more developed method of cooling is Minimum Quantity Lubrication (MQL), where the amount of fluid used is reduced significantly by applying only a highly controlled mist of lubricant in the grinding zone. Two types of MQL fluids were used: HP KOOLKUT 40-an ordinary emulsifiable oil that forms a milky white emulsion and HP SYNTHCOOL 100-a semi-synthetic cutting fluid low in concentration but possesses great thermal properties and it is fluorescent yellow in colour. Both MQL types show excellent heat dissipation, surface finish improvement, and significant resistance to bacterial contamination, making them feasible alternatives for environmentally friendly and high-performing grinding operations.

Tab. 2 Physio-chemical properties of HP KOOLKUT 40

Properties	HP KOOLCUT 40
Colour After Emulsification	Milky White
Kinematic Viscosity at 40 °C, Min, CST	20
Flash Point, COC °C, Min	150
Copper Corrosion at100 °C, Min	1
Cast Iron Corrosion Test, 20:1 Emulsion with 400 PPM Hard Water Max	0/1-1

Tab. 3 Physio-chemical properties of HP SYNTHCOOL 100

Properties	HP SYNTHCOOL 100	
Appearance	Florescent yellow	
Copper Strip Corrosion 3Hr 1 at 100°C, Max	1	
1 :40 in Distilled Water	0/1-1	
1 :40 in Hard Water-200 PPM	0/1-1	

Tables 2 and 3 show the physio-chemical properties of two cooling fluids: HP KOOLKUT 40 and HP SYNTHCOOL 100. HP KOOLKUT 40 is milky white after emulsification, and at 40°C, it manifests a kinematic viscosity of 20 CST, with a flash point of 150°C, while in the corrosion test, it was rated 1 for copper corrosion and 0/1-1 for cast iron corrosion at 20:1 emulsion with 400 PPM hard water. In the case of HP SYNTHCOOL 100, it is fluorescent yellow in appearance, giving a copper strip corrosion rating of 1 after 3 hours at 100°C. Corrosion tests at 1:40 in distilled and hard-water (200 PPM) gave 0/1-1, thus confirming its stable behavior under various conditions.

## 2.3 Experimental Setup and Measurement Techniques

Works on the AHG-60X300 CNC Grinding Machine, conceived and produced by Parishudh Machines Pvt. Ltd., are on samples that can accommodate workpieces with grinding widths of up to 60 mm and center distances of 300 mm. A custom test rig was developed to ensure accurate thermal analysis during grinding and was made up with embedded thermocouples, slip rings for power transfer, and a 10-channel data logger. This system allowed multi-point temperature monitoring of the rotating workpiece under various cooling conditions so that accurate and consistent data could be gathered during the grinding operation.

The experimental set-up, which is a sort of installation for temperature measurement during external cylindrical face, and shoulder grinding operations, is depicted in Fig. l. Viewing various components of the CNC grinding machine superimposed by the temperature-measuring instruments, such as thermocouples and a data logger, it is evident that temperatures are measured in real time as the grinding proceeds.

Table 4 delineates the design specifications of the CNC face and shoulder grinding machine of type AHG-60X300. The main specifications include the maximum workpiece width of 60mm, maximum distance between centers of 300mm, external wheelhead with grinding wheel of size 500mm x 254mm. The machine is operated by a power source of 7.5 kW AC induction motor with a rapid feed of 10m/min, requiring an overall power of 25 kW and weighing 4000 kg making it suitable for precision grinding.

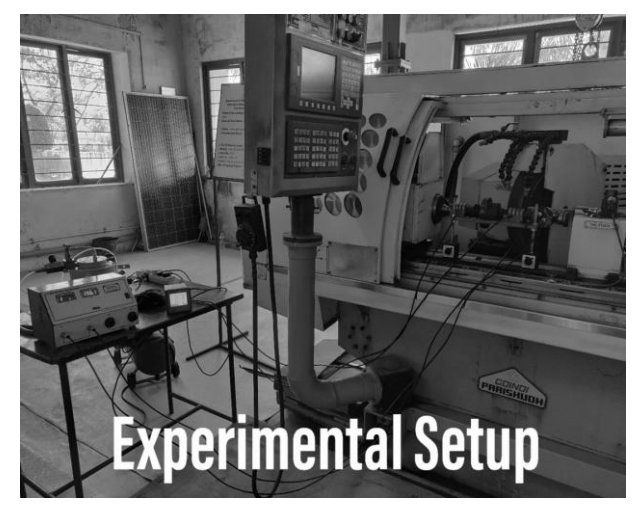


Fig. 1 Experimental Setup for Measuring Temperature in External Cylindrical Face and Shoulder Grinding Operation

**Tab.** 4 Specifications of Face and Shoulder grinding machine used

Item	Specification		
	AHG- 60X300 CNC		
Machine Type	Maximum width of the work piece to be grind=60mm,		
	Maximum Distance between centers = 300mm.		
Manufactures Name	Parishudh Machines Pvt. Ltd.		
Committee	Centre Height: 130mm		
Capacities	Distance between centers: 300mm		
External Wheel Head	Grinding Wheel (OD x ID) = φ500mm X φ 254mm		
External wheel Head	Maximum Width: 60mm		
	Spindle Motor (AC induction Motor): 7.5 Kw		
W 1 II 1 (D 1)	Grinding Speed: 45m/s		
Work Head (Dead)	Spindle Speed (infinitely variable):50 – 650 rpm		
	Spindle motor (AC Servo Motor): 6NM		
	Total Stroke: 200mm		
T. C. 101:1 (X7.A.:)	Rapid Feed rate: 10m/min		
Infeed Slide (X-Axis)	Feed A. C. Servo Motor: 6NM		
	Input Resolution: 0.0001mm		
	Total Stroke: 400mm		
77 11 (77 A · )	Rapid feed rate: 10m/min		
Table (Z-Axis)	Feed A. C. Servo motor: 6NM		
	Input Resolution: 0.001mm		
71 1 C. 1 A 11	Travel: 40mm		
Tail Stock Assembly	Centre: MT 4		
	Coolant Pump Motor: 1.5KW		
General	Total power requirement: 25Kw		
	Total Weight of the machine: 4000kg		

### 3 Methodology

The dataset used for prediction of temperature in cylindrical grinding operations included input features like Depth of Cut, Feed Rate, Work Speed, Wheel Speed, and Cooling Condition. Since cooling condition was a categorical variable with three classes, namely Dry, MQL with HP KOOLKUT 40, and MQL with HP SYNTHCOOL 100, OneHotEncoder encoding was performed to render it interpretable by machine-learning models. To maintain uniformity during the training process and avoid any single feature dominating on account of differences in scale, all input variables were normalized using Standard-Scaler(), thereby converting them into a standard

Gaussian distribution. After preprocessing and removal of incomplete records, the final dataset consisted of 86 samples. The data were then split into training and testing sets using an 80:20 ratio, resulting in 68 samples in the training set and 18 samples in the testing set. Stratified sampling was applied to preserve the distribution of the three cooling condition classes across both subsets, thereby minimizing potential class imbalance and ensuring effective generalization.

### 3.1 Machine Learning Models for Temperature Prediction

### 3.2.1 Random Forest Regressor (RF)

Random Forest Regressor (RF) is an ensemblebased machine-learning model that came into use in this study because of its ability to improve the prediction accuracy through the ensemble technique of combining multiple decision trees [22-24]. Particularly suited for non-linear relationships on complex data sets like those arising in machining operations, RF averts overfitting by prediction averaging of many decision trees and increases generalization in creating a prediction. The performance of the model was finetuned by changing its key hyperparameters: the number of decision trees (n\_estimators) varied between 50 and 200, max depths of each tree (max\_depth) from 5 to 50, and the minimum number of samples required to split an internal node (min\_samples\_split) ranged from 2 to 10. With optimized hyperparameters, the RF model went on to predict grinding temperatures with significant accuracy under different conditions set for the process.

RF: 
$$\hat{y} = \frac{1}{N} \sum_{i=1}^{N} T_i(x)$$
 (1)

### 3.2.2 Gradient Boosting Regressor (GB)

Gradient Boosting Regressor (GB) was selected for its promise in minimizing bias and variance from a perspective of sequential learning, where trees are built one after the other [22-24]. The GB method sequentially constructs trees in a way that each new tree is trained to correct the residual errors of the aggregate ensemble of previous trees-a property that allows further adjustments in GB for model accuracy incrementally, rewarding the method against complex regression challenges like temperature prediction in grinding operations. The engine was modeled through tuning processes in which the n\_estimators were varied from 100 to 300, learning\_rate from 0.005 to 0.2, max\_depth from 4 to 50, subsample from 0.6 to 1.0, and min\_samples\_split from 2 to 10. These settings provided a balance between training capacity and avoiding overfitting.

GB: 
$$\hat{y}_m = \hat{y}_{m-1} + \eta \cdot f_m(x)$$
 (2)

#### 3.2.3 Artificial Neural Networks (ANN)

Artificial Neural Networks (ANNs) were to model complex non-linear interactions among input features through the Multi-Layer Perceptron Regressor (MLPRegressor) [22-24]. The ANN design closely tracked the intricate patterns of the dataset; the tree-based ones would never unlock. The network architecture consisted of three hidden layers with several neurons in each layer being 200, 200, and 100, respectively, ensuring deep learning turns. The introduction of non-linearities was performed by the tanh activation function, whereas weight optimization was done with lbfgs solver. In addition to that, the learning rate was adaptively modified to suit different gradient behaviours during training, up to 10,000 iterations being taken to ensure proper convergence of the mo-

del. This setting allowed the ANN to perform remarkably well in prediction scenarios where slight or even complex interactions among features are involved.

ANN: 
$$y^{(l)} = f(W^{(l)} \cdot y^{(l-1)} + b^l)$$
 (3)

### 3.2 Hyperparameter Optimization using Bayesian Search

Hyper-parameter tuning of all three machine learning models was performed with Bayesian Optimization, leveraging the probabilistic approach to optimize the search space effectively and decrease the prediction error. The performance of the models was evaluated during this process by three important metrics: the squared difference between the predicted value and true value, averaged over all observations (Mean Squared Error, MSE); the proportion of variance in the target variable accounted for by the model (R<sup>2</sup> Score); and the average magnitude of the error in the predictions (Mean Absolute Error; MAE). Convergence was decided when either validation loss plateaued or the validation accuracies crossed the defined thresholds over 20 consecutive iterations, ensuring best model performance with no overfitting.

### 3.3 Genetic Algorithm for Process Optimization

The grinding process was optimized by a genetic algorithm. The aim of the genetic algorithm is to yield the minimum grinding temperature through the most favourable combination of process parameters and cooling methods. The developed fitness function was based on the temperature prediction by the trained model.

The Genetic algorithm (GA) with a population size of 20 individuals per generation was employed to discover the optimal machining parameters and cooling condition, incorporating tournament selection in the design to maintain robustness, ensuring survival for high-quality solutions. Blend Crossover (CX) and Gaussian mutation operators were used in selecting the appropriate genetic operators to increase genetic diversity and diminish convergence to local minima. The GA, very iteratively running through many generations of evolution work, developed the best configuration to minimize grinding temperature.

This flowchart in Fig. 2 explains the entire process of predicting and optimizing the grinding process. It begins with the preprocessing of data, i.e., encoding and scaling of input features, and the splitting of data into training and testing datasets. Case modeling and training employ methods such as Random Forest, Gradient Boosting, and Artificial Neural Networks to predict grinding temperatures. Hyperparameter tuning and genetic algorithms are implemented in the final step to optimize other process parameters such as cooling conditions for greater efficiency and accuracy in the grinding process.

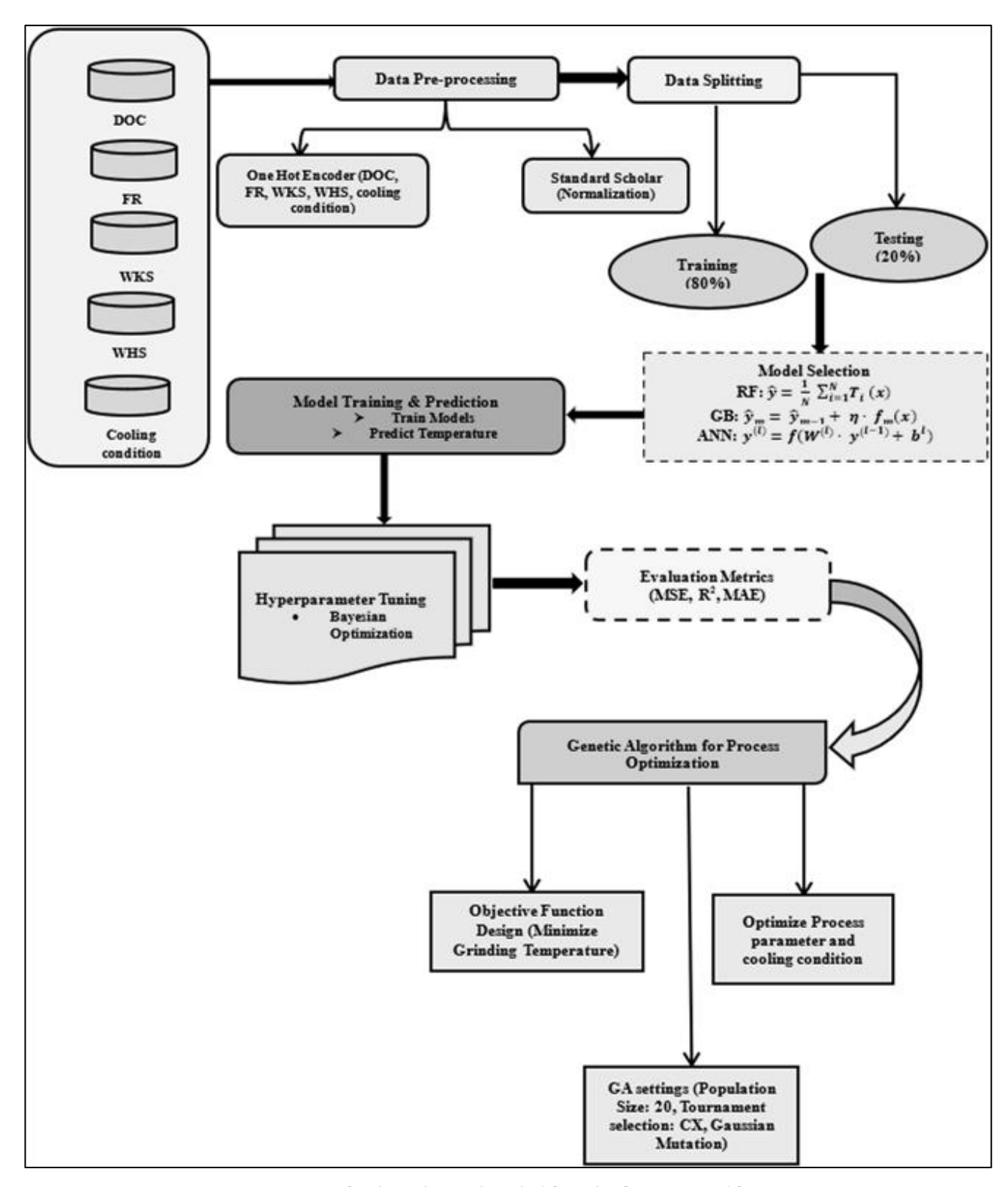


Fig. 2 Flowchart of research methodology of RGA\_NN model

#### 4 Results and Discussion

This section of the paper discusses the experimental results obtained using machine-learning models employed for temperature prediction in cylindrical grinding operations. Various evaluation metrics-correlation analysis, residual analysis, confusion matrices, and performance comparison of the models-are discussed in detail.

### 4.1 Correlation Analysis

Constructing a correlation matrix helps to study the inter-relationships among input features (depth of cut, feed rate, work speed, wheel speed, and cooling conditions) and output variables (temperature at the face and shoulder). As shown in Fig. 3, the heatmap employs a color scale that varies within a continuous range of hues as they traverse from strong red to strong blue color, with lighter, less intense colors used to mark positive and negative correlations. The heatmap shows that temperature at the face and shoulder is strongly positively correlated (0.81-0.84) with cooling conditions, especially with the MQL using HP

SYNTHCOOL 100, being most effective for temperature reduction as compared to other cooling techniques. To yield a clearer understanding of the given data, an elaborate explanation concerning the color scale and interpretation with respect to accuracy of model prediction is needed.

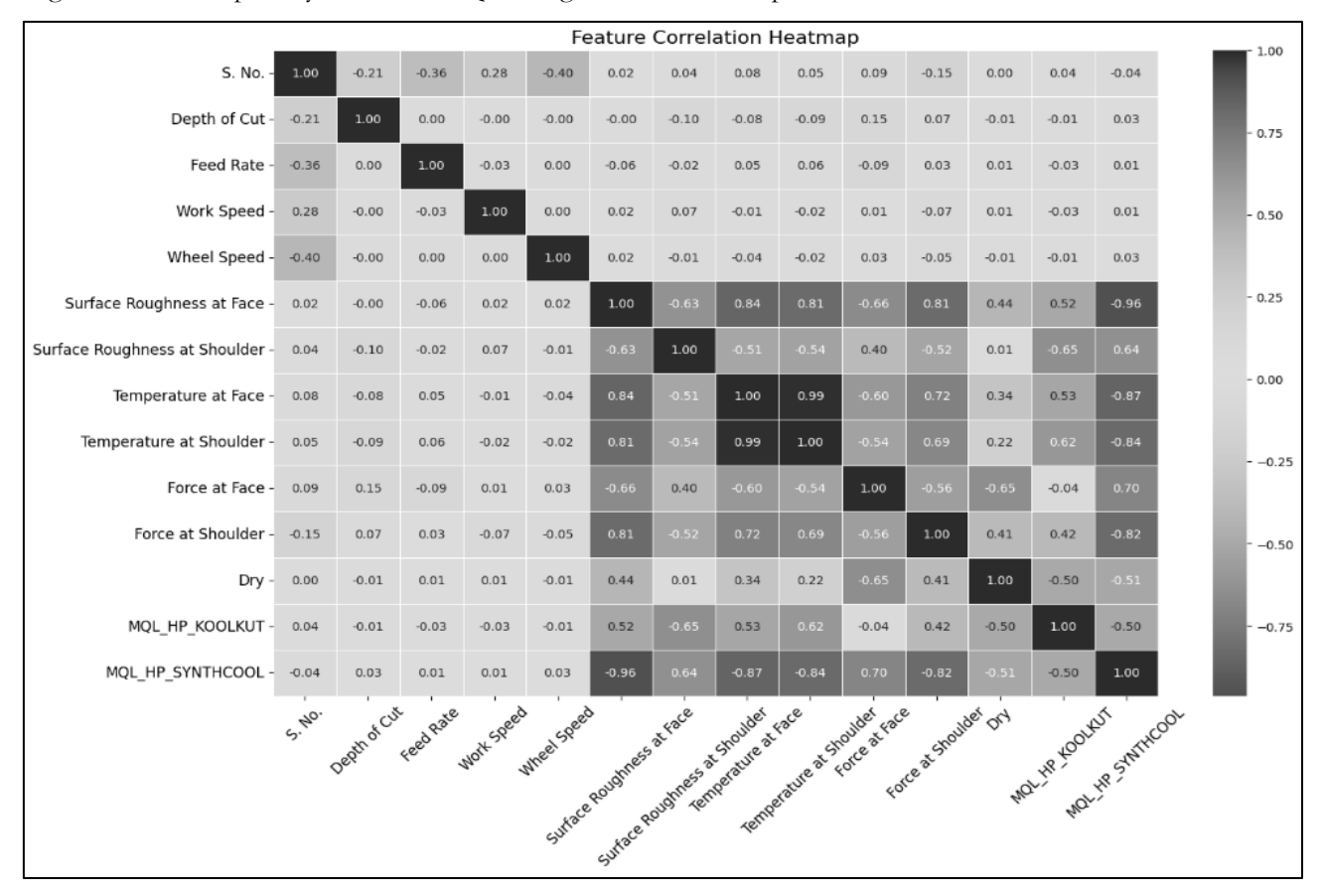


Fig. 3 Feature Correlation Heatmap

There was a strong correlation between the face and shoulder workpiece temperatures, with coefficients in the range of ~0.81 to 0.84, which signifies that if one temperature increases, the other typically follows. Of all variables, the cooling condition was the most dominant. Minimum Quantity Lubrication (MQL) with HP SYNTHCOOL 100 resulted in a substantially lower temperature compared with either dry or any other cooling conditions. Feed Rate and Work Speed were shown to moderately influence temperature change, which represented a key quantity for thermal control during the grinding operation.

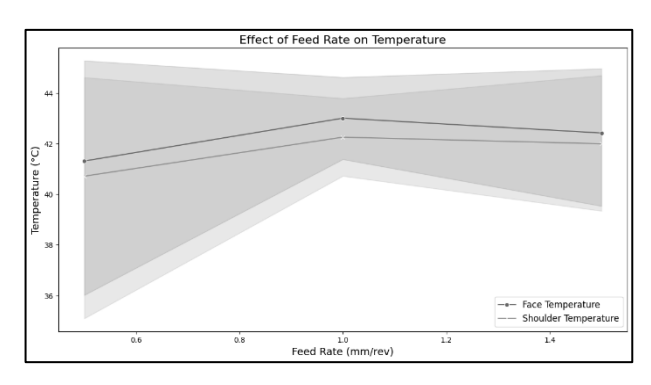
### 4.2 Relationship Analysis in Pairs

This plot was created which visualizes the distribution and interaction between input features and the target variable.

Fig. 4 shows the effect of feed rate on temperature at the face and shoulder during grinding. The graph depicts a more or less steady rise of temperature at the face with increasing feed rate, while the shoulder temperatures vary almost independently from the feed

rate, suggesting that the face temperature is much affected by the feed rate. The shaded regions represent the margin of error or difference in temperature data at every feed rate, presenting an idea of the extent of temperature variation in the measurements. An elaborated explanation of this variability would better illuminate the feed rate-temperature relationship, thereby giving greater and enhanced insight into the mechanism of the grinding process.

Fig. 5 depicts the variations in temperature at the face and shoulder as influenced by the depth of cut. Aprove heighting temperatures at both locations decline with an increase in the depth of cut; the variation in temperature is higher in the face than the shoulder. This indicates that the cooling effect of the depth of cut is more profound on the face of the workpiece. The shaded regions depict the variation in temperature data for different depths of cut. This further goes to show how deeper cuts are able to cool the face better and should be studied further to stress the practical importance of utilizing cutting depth during machining operations for better thermal management.



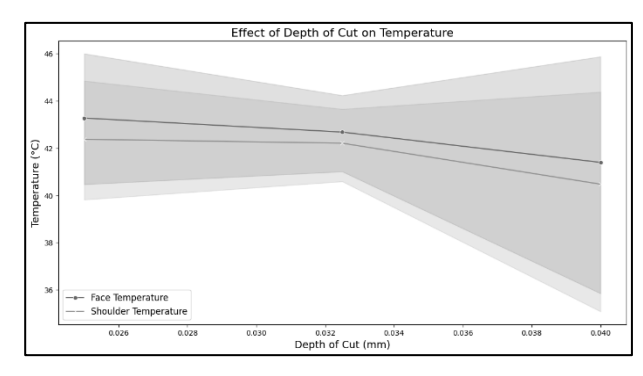


Fig. 4 Effect of Feed Rate (FR) on Temperature

Fig. 5 Effect of Depth of Cut (DOC) on Temperature

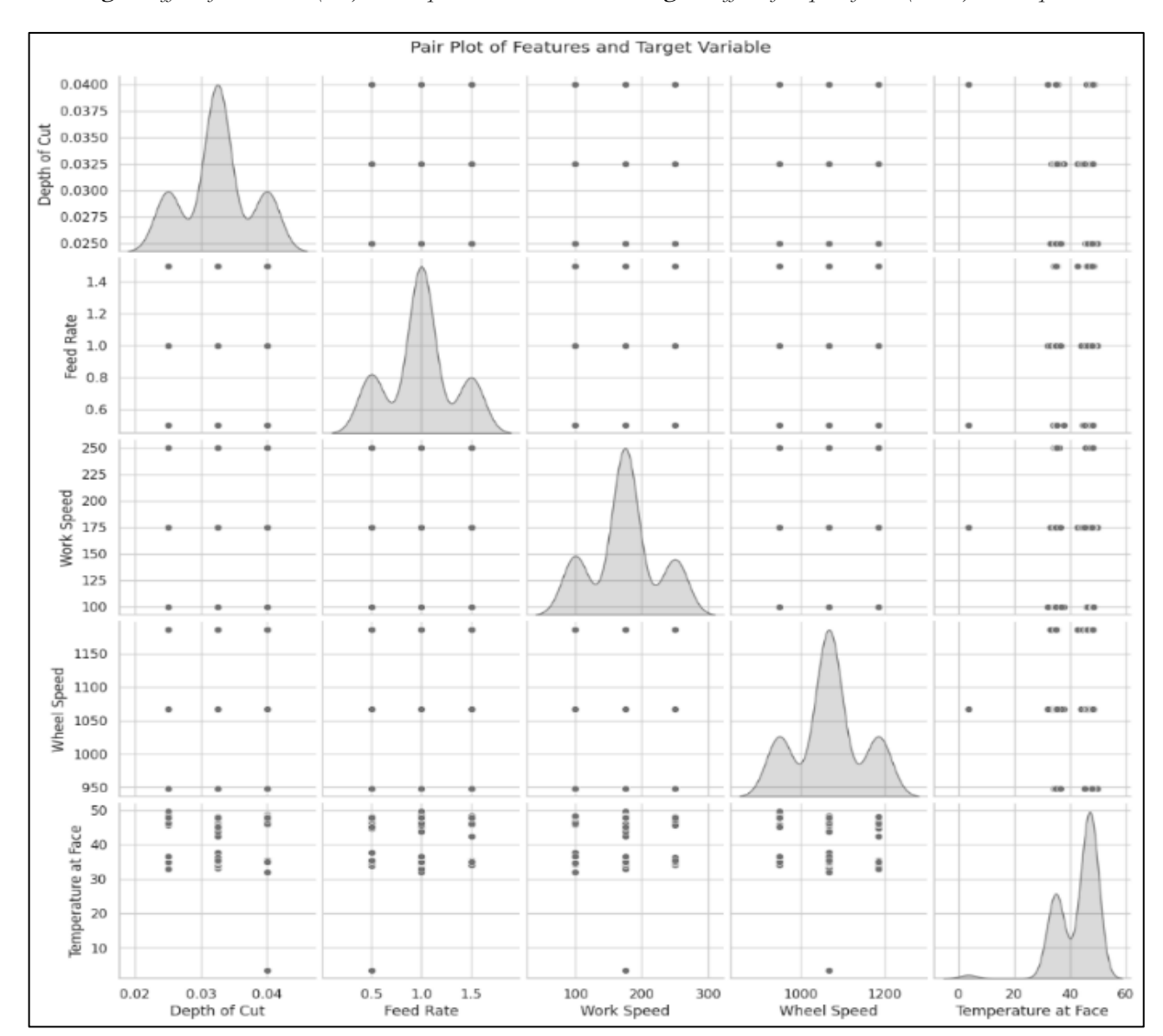


Fig. 6 Pair Plot of features and Target Variable

Fig. 6 shows the pair plot showing the relationships between features (Depth of Cut, Feed Rate, Work Speed, and Wheel Speed) with the target variable temperature at face. The pair plots comprise scatter plots between one feature and another with distribution distribution histograms on the diagonal. These scatter plots show that there are trends between temperature

at the face and features like Feed Rate and Work Speed while the histograms show the feature-wise distribution within the dataset. The trends in these scatter plots must be explained deeply, especially about how feed rate and wheel speed relate to face temperature, as it would give deep insight into the mechanistics of the grinding process.

It was found that the distributions of parameters could be analysed with respect to their depth of cut and feed rate, which play different roles in temperature development during grinding. The localized heat generation would be due to changes in depth during cutting, while the feed rate would account for the total thermal load for a certain amount of time. Great work speed and wheel speed, in some of the experimental cases, lowered the temperature. This may indicate that these factors could enhance the heat dissipation process and improve the overall thermal behavior during grinding. These findings adequately emphasize the precision of balance of input parameters to afford heat production management.

### 4.3 Residual Analysis

Different models are evaluated by analysing upright residual plots. The box plot of residuals for RF, Gradient Boosting, and ANN is in Fig. 7; the plot gives us a glance on the error ranges of the different methods: From this plot, we observe that Random Forest and Gradient Boosting models observe lesser outliers with the ANN model having an open-ended spread of residuals, implying a high variance in its predictions. With respect to residuals, a more balanced residual distribution is shown by the Random Forest model, hence making it more reliable. An explanation of the importance of these residuals and how they affect the prediction accuracies of the models would help in defining further aspects of model performance.

The diverse nature of the residual analysis stands out in contrasting the performances of different machine learning models. The Random Forest model exhibited reasonably balanced residuals with lower variance, showing that its predicted results can be trusted across the dataset. The Gradient Boosting model, on the other hand, displayed a slightly wider scatter of the residuals, suggesting minor inconsistencies in predictions that could be arising due to complex interdependencies in the data. The Artificial Neural Network (ANN), meanwhile, exhibited the highest residual variance, indicating that the model might require additional tuning for greater stability and generalized performance. Such deductions suggest that Random Forest is equally reinforced as the strongest model in this research.

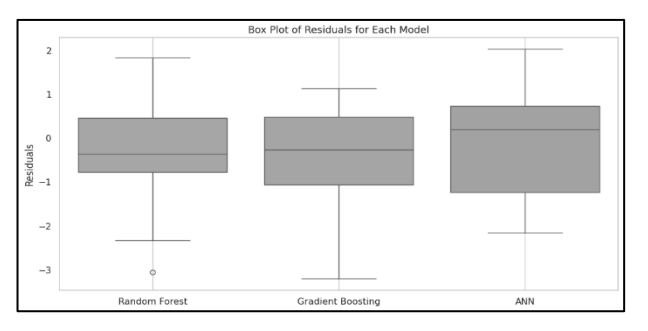


Fig. 7 Box plot of residuals for each model

### 4.4 Residual Distribution Across Models

Fig. 8 shows residual histograms for the RFs, GBs, and ANN models for error and prediction trend analysis. The histograms reveal that the Random Forest model residuals were tightly distributed about zero and, hence, well-predicted; whereas the ANN residuals were scattered, indicating that more optimization is required. Gradient Boosting also showed more variation in errors when compared to the Random Forest model. Understanding these residual trends and the consequences for model performance will better inform model utility and areas for further improving the model.

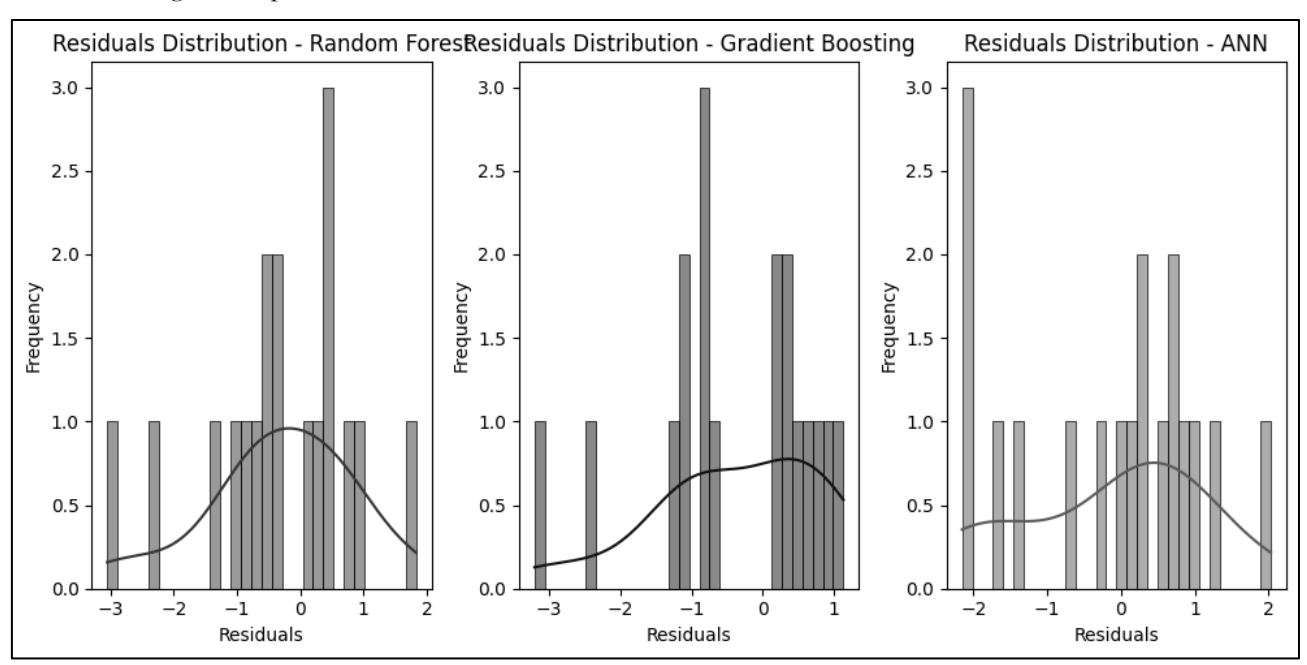


Fig. 8 Residuals distribution for each model

Refitting of the residual distribution indicated substantial variation among the models under consideration. The Random Forest model presented a concentrated distribution of residuals about the zero line; hence, making predictions that were largely correct with little bias from the mean. In contrast, the Gradient Boosting model presented a slight skewness in its residuals, which implied some level of over-predictions displayed by the model especially in the higher temperature range. On the contrary, scattered residuals of ANN suggested wide variability in prediction, warranting further optimization improvements for accuracy and consistency. These findings indicate that while Random Forest almost perfectly captured the phenomenon being modelled, some further tuning and refinement apply to Gradient Boosting and ANN.

### 4.5 Model Comparison Metrics

The analysis of the performance of the models affirmed that Random Forest had the best performance, having the least Mean Squared Error (MSE) and the highest R<sup>2</sup> score, with a direct implication that it had a better ability in predicting deviation of temperature with accuracy and least error. Gradient

**Tab. 5** Performance of the models

Boosting had a rather good performance overall, but because it exhibited a slightly higher error margin than Random Forest, which leaves it up for further optimization. Once properly optimized, ANN showed competitive performance, however, with higher residual variance, suggesting that there is still scope for improvement in terms of consistency in predictions even after optimization. For the models to be assessed, being on slightly more of the efficiency aspect, MSE and R<sup>2</sup> scores were in comparison, with Random Forest emerging as the most reliable among all; Gradient Boosting and ANN holding promise yet should be tuned in further for better performance. Table 5 provides a comparison of the Mean Squared Error (MSE) and R<sup>2</sup> scores for the three machine learning models: RF, GB, and ANN. RF has the lowest error and the highest goodness of fit, making it the best-suited model for the temperature prediction task. An appropriate explanation about the statistical significance of the results, especially regarding how MSE and R<sup>2</sup> are calculated and what they mean for model validation, would have undoubtedly improved the value of this table.

2 de la cijarmanta aj instrumanta	5. C 1 cryot matrice by the models		
Model	MSE (Lower is better)	R <sup>2</sup> Score (Higher is better)	
Random Forest	1.3307	0.9631	
Gradient Boosting	1.4669	0.9593	
Artificial Neural Network	1.5302	0.9576	

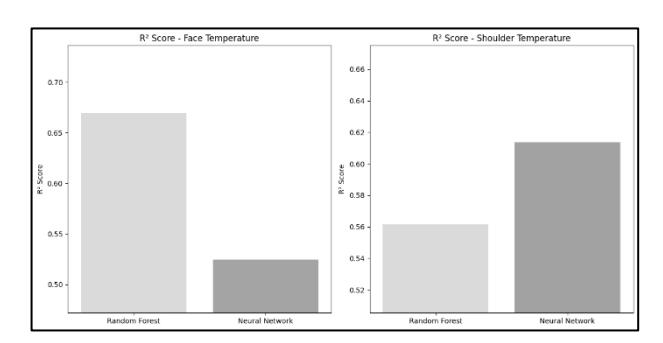
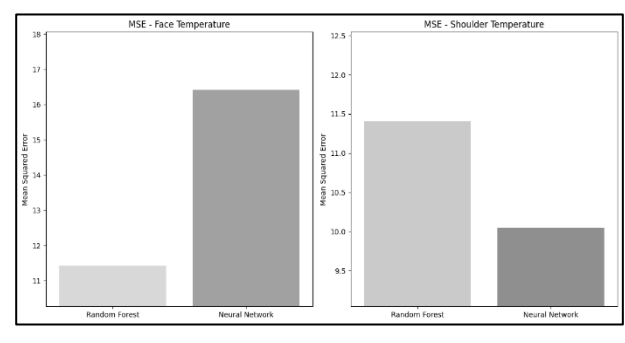


Fig. 9 R<sup>2</sup> score comparison of Temperature at face and shoulder for RF and ANN

Fig. 9 to 11 present a comparison of the three machine learning models Random Forest (RF), Gradient Boosting (GB), and Artificial Neural Network (ANN) to model grinding temperature at face and shoulder. Fig. 9 shows that RF performs better than ANN in modeling face temperature, with ANN doing better for the shoulder temperature. Fig. 10 presents the MSE values that point to slightly lesser errors of the ANN in shoulder temperature predictions, hinting that ANN can grasp some patterns better than RF,

even if RF stays better overall. Fig. 11 shows MSE and R<sup>2</sup> scores for all three models. It is so evident that RF and ANN behave equally well in MSE and R<sup>2</sup>, while GB suffers from high MSE and low R<sup>2</sup> scores, basically meaning that RF is the most dependable model for both temperature predictions. It would be worth more discussing the practical value of these differences in model performance from the potential application viewpoint of the grinding process and lowering errors.



**Fig. 10** MSE values comparison of temperature at face and shoulder for RF and ANN

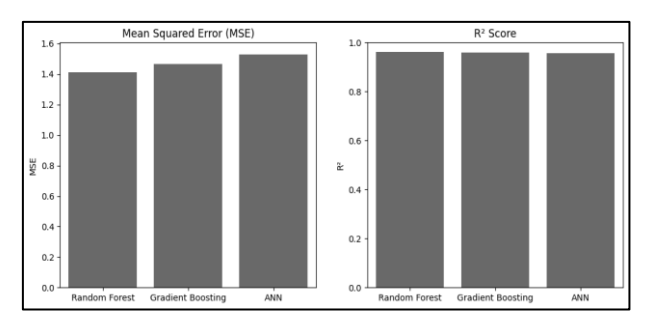


Fig. 11 MSE values comparison of temperature at face and shoulder for RF, GB, ANN

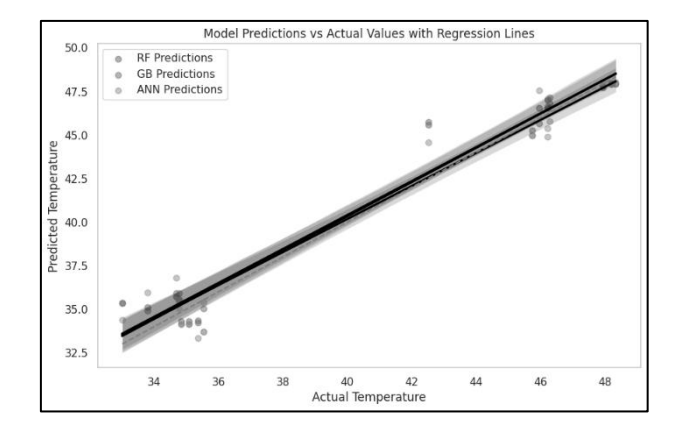


Fig. 12 Model prediction vs actual values with regression lines for all three models (RF, GB, ANN)

Fig. 12 depicts the predicted-versus-observed comparisons for RF, GB, and ANN, with regression lines closely fit to the observations for all three models. This shows that all models have performed well in predicting temperature values, hence are high in accuracy. This strong agreement of the regression lines with the actual data underscores the sound capacity of the models in temperature prediction. In order to enrich the explanations of model performance, it would be helpful to discuss in greater detail how these regression lines were created and what their significance is in the context of validating the models' predictive ability.

### 4.6 Statistical Significance Analysis

To assess whether the observed differences in predictive performance across Random Forest (RF), Gradient Boosting (GB), and Artificial Neural Network (ANN) models were statistically significant, an ANOVA was performed on the residual distributions, followed by pairwise paired t-tests with Holm–Bonferroni correction. The one-way ANOVA yielded F = 0.3235, p = 0.7251, indicating that the variance in residuals across the three models was not statistically significant. Subsequent pairwise comparisons further confirmed the absence of significance at  $\alpha = 0.05$  (Fig. 12).

**Tab.** 6 Statistical significance analysis of model residuals using pairwise paired t-tests with Holm–Bonferroni correction

Comparison	Raw p-value	Adjusted p-value	Significant ( $\alpha = 0.05$ )
RF vs GB	0.1376	0.4128	No
GB vs ANN	0.2325	0.4651	No
RF vs ANN	0.9567	0.9567	No

These results confirm that while RF achieved slightly better predictive accuracy in terms of MSE and R<sup>2</sup>, the differences among the three models are not statistically significant at the 95% confidence level.

This suggests that all three algorithms are capable of capturing the dominant thermal behavior trends within the available dataset, though tree-based models exhibit relatively stronger robustness.

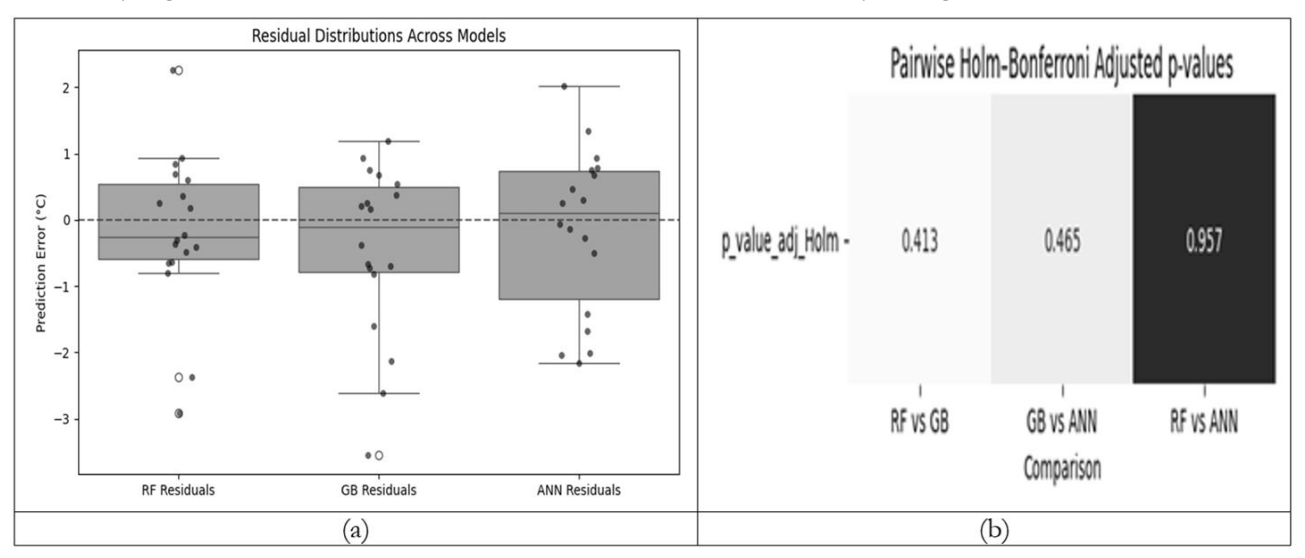


Fig. 13 Pairwise statistical comparison of model residuals (Holm–Bonferroni adjusted p-values)

Figure 13 (a) presents the distribution of residuals (prediction errors) for the Random Forest (RF), Gradient Boosting (GB), and Artificial Neural Network (ANN) models. All three models show residuals scattered around zero, with no evident systematic bias. While ANN exhibits slightly larger spread compared to RF and GB, the overall distributions are overlapping, suggesting comparable predictive accuracy.

Figure 13 (b) shows the pairwise p-values from paired t-tests with Holm–Bonferroni correction. None of the adjusted p-values fall below the significance threshold ( $\alpha=0.05$ ), indicating that the performance differences among RF, GB, and ANN are not statistically significant. This means that although RF and GB tend to have slightly lower error dispersion than ANN, the differences could be attributed to random variation rather than true model superiority.

### 5 Conclusion and Future Scope

This study successfully integrates machine learning models and traditional optimization methods to achieve precision and accuracy in cylindrical grinding operations. The results signify that the Random Forest (RF) model, with an R2 score of 0.96, surpasses Gradient Boosting (GB) and Artificial Neural Networks (ANN) in predicting grinding temperatures-i.e., better prediction. Bayesian optimization and genetic algorithms were applied to attain optimization of grinding parameters and cooling methods, further reducing grinding temperatures and improving surface quality. Among all cooling methods studied, MQL with HP SYNTHCOOL 100 had the greatest potential for temperature control compared to dry cooling methods in terms of energy consumption and environmental impact. Thus, the optimization minimized not only thermal damage but also contributed to a greener and more efficient manufacturing process. Further, the study exhibits how AI-based techniques can enhance machining performances, conserve resources, and improve surface integrity.

Future scope may include enlarging the data set and testing the methodology for differing machining operations to know the generic adaptability of the models. Optimization of machine learning models can be pursued further, and newer cooling methods can be investigated towards improving the robustness of the models as well as reducing the residual stresses and surface defects. With such advances, this research may lead to the application of such methods in high-precision green manufacturing.

### Acknowledgement

This article was co-funded by the European Union under the REFRESH – Research Excellence For REgion Sustainability and High-tech Industries project number CZ.10.03.01/00/22\_003/0000048 via the Operational Programme Just Transition and has been done Students Grant Competition SP2025/062 "Specific research on progressive and sustainable production technologies" and SP2025/063 "Specific research on innovative and progressive manufacturing technologies" financed by the Ministry of Education, Youth and Sports and Faculty of Mechanical Engineering VŠB-TUO.

### References

- [1] WEI, C., HE, C., CHEN, G., SUN, Y., & REN, C. Material removal mechanism and corresponding models in the grinding process: A critical review. *Journal of Manufacturing Processes*, Vol. 103, 2023, pp. 354-392. https://doi.org/10.1016/j.jmapro.2023.08.045
- [2] JEDAMSKI, R., KUHLMANN, G., RÖBLER, M., KARPUSCHEWSKI, B., DIX, M., & EPP, J. Towards developing a control of grinding processes using a combination of grinding power evaluation and Barkhausen noise analysis. *Production Engineering*, Vol. 18, No. 2, 2024, pp. 339-351. https://doi.org/10.1007/s11740-023-01247-x
- [3] CHARDE, M.M., NAJAN, T.P., CEPOVA, L., JADHAV, A.D., RASHINKAR, N.S., & SAMAL, S.P. Predictive modelling of surface roughness in grinding operations using machine learning techniques. *Manufacturing Technology*, Vol. 25, No. 1, 2025, pp. 14-23. https://doi.org/10.21062/mft.2025.006
- [4] CHARDE, M.M., BHALERAO, Y.J., & RASHINKAR, N.S. Method for temperature measurement to determine the temperature variations in face and shoulder grinding contact arc. *International Journal of Advanced Research in Engineering and Technology*, Vol. 11, No. 11, 2020, pp. 218. https://doi.org/10.34218/IJARET.11.11.2020 218
- [5] SCHIEBER, C., HETTIG, M., ZAEH, M.F., & HEINZEL, C. Evaluation of approaches to compensate the thermo-mechanical distortion effects during profile grinding. *Procedia CIRP*, Vol. 102, 2021, pp. 331-336. https://doi.org/10.1016/j.procir.2021.09.057
- [6] LEE, S., CHEN, Z., LUO, Y., LI, X., LU, M., HUANG, Z.H., & HUANG, H. Enhanced prediction accuracy in high-speed grinding of brittle materials using advanced machine learning techniques. *Journal of Intelligent Manufactu*ring, 2024, pp. 1-45. https://doi.org/10.1007/s10845-024-02532-x

- [7] REN, X., HUANG, X., CHAI, Z., LI, L., CHEN, H., HE, Y., & CHEN, X. A study of dynamic energy partition in belt grinding based on grinding effects and temperature dependent mechanical properties. *Journal of Materials Processing Technology*, Vol. 294, 2021, pp. 117112. https://doi.org/10.1016/j.jmatprotec.2021.117112
- [8] GAO, B., BAO, W., JIN, T., CHEN, C., QU, M., & LU, A. Variation of wheel-work contact geometry and temperature responses: thermal modeling of cup wheel grinding. *International Journal of Mechanical Sciences*, Vol. 196, 2021, pp. 106305. https://doi.org/10.1016/j.ijmecsci.2021.10630
- [9] ZHOU, K., DING, H., STEENBERGEN, M., WANG, W., GUO, J., & LIU, Q. Temperature field and material response as a function of rail grinding parameters. *International Journal of Heat and Mass Transfer*, Vol. 175, 2021, pp. 121366. https://doi.org/10.1016/j.ijheatmasstransfer.2021.121366
- [10] MA, Z., WANG, Q., CHEN, H., CHEN, L., MENG, F., CHEN, X., et al. Surface prediction in laser-assisted grinding process considering temperature-dependent mechanical properties of zirconia ceramic. *Journal of Manufacturing Pro*cesses, Vol. 80, 2022, pp. 491-503. https://doi.org/10.1016/j.jmapro.2022.06.019
- [11] ZHONG, Y., DAI, Y., XIAO, H., & SHI, F. Experimental study on surface integrity and subsurface damage of fused silica in ultra-precision grinding. *The International Journal of Advanced Manufacturing Technology*, Vol. 115, No. 11, 2021, pp. 4021-4033. https://doi.org/10.1007/s00170-021-07439-y
- [12] YANG, J., ZHENG, Y., & WU, J. Towards sustainable production: An adaptive intelligent optimization genetic algorithm for solid wood panel manufacturing. *Sustainability*, Vol. 16, No. 9, 2024, pp. 3785. https://doi.org/10.3390/su16093785
- [13] SEN, B., DEBNATH, S., & BHOWMIK, A. Sustainable machining of superalloy in minimum quantity lubrication environment: leveraging GEP-PSO hybrid optimization algorithm. *The International Journal of Advanced Manufacturing Technology*, Vol. 130, No. 9, 2024, pp. 4575-4601. https://doi.org/10.1007/s00170-024-12962-9
- [14] LIU, T., YE, X., CHENG, L., HU, Y., GUO, D., HUANG, B., LI, Y., & SU, J. Intelligent pressure monitoring method of BP neural

- network optimized by genetic algorithm: A case study of X Well Area in Yinggehai Basin. *Processes*, Vol. 12, No. 11, 2024, pp. 2439. https://doi.org/10.3390/pr12112439
- [15] ROSTAMZADEH-RENANI, R., JASIM, D.J., BAGHOOLIZADEH, M., ROSTAMZADEH-RENANI, M., ANDANI, H.T., SALAHSHOUR, S., & BAGHAEI, S. Multi-objective optimization of rheological behavior of nanofluids containing CuO nanoparticles by NSGA II, MOPSO, and MOGWO evolutionary algorithms and Group Method of Data Handling Artificial neural networks. *Materials Today Communications*, Vol. 38, 2024, pp. 107709. https://doi.org/10.1016/j.mtcomm.2023.1077
- [16] SEN, B., KUMAR, R., KANABAR, B., KEDIA, A., KUMAR, A.V., & BHOWMIK, A. Comparative analysis of NSGA-II and TLBO for optimizing machining parameters of Inconel 690: A sustainable manufacturing paradigm. *Journal of Materials Engineering and Performance*, 2024, pp. 1-16. https://doi.org/10.1007/s11665-024-10539-x
- [17] CAO, Y., SU, F., ANTWI-AFARI, M.F., LEI, J., WU, X., & LIU, Y. Enhancing mix proportion design of low carbon concrete for shield segment using a combination of Bayesian optimization-NGBoost and NSGA-III algorithm. *Journal of Cleaner Production*, Vol. 465, 2024, pp. 142746. https://doi.org/10.1016/j.jclepro.2024.14274
- [18] NWANKITI, U. S., OLUWO, A., OYEKEYE, M. O., RAJAN, J., JOSE, S., KADADEVARMATH, R., ... & ODUDARE, S. O. Analysis of the thermal friction drilling process for effective parametric choice on the drilling of aisi 304 stainless steel using the fuzzy ahp-moora method. *Kufa Journal of Engineering*, Vol. 15, 2024, pp. 4. https://doi.org/10.30572/2018/KJE/150411
- [19] ZAMAN, P.B., TUSAR, M.I.H., & DHAR, N.R. Multi-criteria process optimization for better performance of grinding AISI 1060 hardened steel using different hybrid taguchibased MCDM methods. International *Journal on Interactive Design and Manufacturing* (IJIDeM), Vol. 19, No. 7, 2025, pp. 5313-5330. https://doi.org/10.1007/s12008-024-02114-4
- [20] TOUATI, S., BOUMEDIRI, H., KARMI, Y., CHITOUR, M., BOUMEDIRI, K.,

- ZEMMOURI, A., & FERNANDES, F. Performance analysis of steel W18CR4V grinding using RSM, DNN-GA, KNN, LM, DT, SVM models, and optimization via desirability function and MOGWO. *Heliyon*, Vol. 11, No. 4, 2025, pp. e42640. https://doi.org/10.1016/j.he-liyon.2025.e42640
- [21] SREDANOVIC, B., CICA, D., BOROJEVIC, S., TESIC, S., & KRAMAR, D. Optimization of superalloy Inconel 718 micro-milling process by combined Taguchi and multi-criteria decision making method. *Journal of the Brazilian Soci*ety of Mechanical Sciences and Engineering, Vol. 46, No. 7, 2024, pp. 423. https://doi.org/10.1007/s40430-024-04996-7
- [22] KALITA, K., CHAKRABORTY, S., GAUTAM, P., PETRŮ, J., & SAMAL, S.P. Machine Learning-Based Predictive Modelling

- of Laminated Composites. *MM Science Journal*, Vol. 2025, No. 1, 2025, pp. 8169-8175. https://doi.org/10.17973/MMSJ.2025\_03\_20 25007
- [23] BURANDE, D.V., KALITA, K., GUPTA, R., KUMAR, A., CHOHAN, J.S., & KUMAR, D. Machine Learning Metamodels for Thermo-Mechanical Analysis of Friction Stir Welding. *International Journal on Interactive Design and Manu*facturing, Vol. 19, No. 1, 2025, pp. 597-615. https://doi.org/10.1007/s12008-024-01871-6
- [24] KALITA, K., GHADAI, R.K., ČEP, R., & JANGIR, P. Enhancing Welding Quality Through Predictive Modelling Insights from Machine Learning Techniques. *MM Science Journal*, Vol. 2024, No. 6, 2024, pp. 7897-7902. https://doi.org/10.17973/MMSJ.2024\_12\_20 24124